Influence of changing ground conditions on deformations near the tunnel face

J.S. Jeon[a], C.D. Martin[b,*], D.H. Chan[b], J.S. Kim[b]

[a]Korea Water Resources Corporation(KOWACO), 462-1, Jeonmin-dong, Yusung-gu, Daejon, KOREA, 305-730

[b]Dept. Civil & Environmental Engineering, University of Alberta, Edmonton, Alberta, Canada T6G 2G7

[c]Hyundai Development Company, Seoul, Korea

Draft 2004 Aug 27

Abstract

Tunnel construction frequently makes use of radial displacements to monitor tunnel support performance, particulary in complex ground conditions. In recent years absolute displacement monitoring methods have replaced the more traditional radial convergence measurements. It has been suggested by Schubert and Budil [1] that these near-face displacements could also be used to forecast the tunnel conditions ahead of the advancing tunnel face. This paper presents the results from a series of detailed three-dimensional analyses in varying ground conditions, which compares vertical (radial) displacements measured at the roof, vector orientations associated with these roof displacements and tunnel face displacements (extrusion). These numerical results suggest that in all cases vector orientation provided additional information not obtained from traditional radial displacements or face extrusion. If interpreted correctly the vector orientations could provide advanced warning of changing ground conditions in the vicinity of the tunnel face.

Keywords: Tunnel deformations, face extrusion, convergence, modelling

1. Introduction

Since the introduction of the New Austrian Tunnelling Method (NATM) by Rabcewicz [2] and the "Observational Design Method" by Peck [3] deformation monitoring has become a fundamental component of modern tunnel construction. In practice, deformation monitoring for most tunnelling situations usually implies radial convergence monitoring because of the well established relationships between convergence and tunnel stability [4]. These relationships have been established using the concepts first proposed by Fenner [5] based upon the development of a plastic zone surrounding the tunnel (Fig. 1). In the ground-support interaction concept in Fig. 1 the relationship between radial displacements and support pressure follows the curve $A-B$ with stability being achieved at B. Knowing if stability has been achieved can readily be determine by monitoring the radial displacements.

In the original ground-support interaction concept, the behaviour of the tunnel face was ignored. However, as illustrated in Fig. 1 considerable radial displacements occurs ahead of the tunnel face. Lunardi et al. [6] and Lunardi [7] have proposed that controlling the deformations associated with the tunnel face is an important factor in controlling the overall stability of the tunnel. Typical radial deformations and the deformations occurring near a tunnel face are illustrated in Fig. 2. Hoek [8] showed using an axi-symmetric numerical model that these face deformations tend to follow the trend of the radial displacements and that the face deformations were approximately 70% of the radial defor-

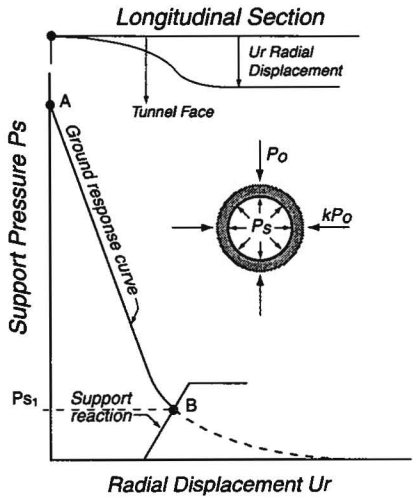

Fig. 1: Ground-support interaction illustrating the relationship between radial displacement and tunnel support.

*Corresponding author.
Tel: +1 (780) 492-2332, Fax: +1 (780) 492-8198
Email: dmartin@civil.ualberta.ca

mations for a wide range of tunnelling conditions where a plastic zone develops.

During the last decade, several examples have been reported where traditional tunnel convergence have been replaced with geodetic methods to determine the three-dimensional displacement patterns of the tunnel roof and in some cases the tunnel face [9, 10]. In these cases, where three-dimensional displacements were measured, the results indicated that the rock mass conditions, ahead of the tunnel face, significantly influenced the orientation of the displacement vectors in space. For example, Schubert and Budil [1] reported that the trend of crown settlement did not indicate changing ground condition ahead of the tunnel face, while the changes in vector orientation of the crown displacements, expressed as the ratio of longitudinal displacements to vertical settlements (L/S), correlated with zones of different stiffness ahead of the tunnel face. This approach which has received limited application holds considerable promise, if changes to ground conditions ahead of the tunnel face can be detected with confidence.

This paper presents the results of three-dimensional numerical simulations carried out to evaluate spatial displacement in the crown and tunnel face for the condition where a relatively large tunnel is advanced towards weak ground. The sensitivity of the solution to, rock mass characteristics, far-field stress and geometry of the contact, is evaluated.

2. Displacement monitoring

2.1. Tunnel face extrusion

Lunardi [7] has shown that the deformations of the tunnel face can be a useful indicator to evaluate the ground response. In Lunardi's approach, deformations associated with the tunnel excavation are classified as: (1) pre-convergence, face extrusion, and (3) radial convergence (Fig. 3). The main concept of this approach is that the stability of ground ahead of the tunnel face plays a fundamental role in controlling the deformation response of the tunnel. As a result, particular attention is paid to the behavior of the tunnel face and not just tunnel convergence, as is normally done.

Lunardi [7] classed the deformation response of the ground in the vicinity of the tunnel face as: elastic behavior, elasto-plastic behavior or collapse behaviour (Fig. 3). Lunardi concluded that there was a direct linkage between the failure of the core and the collapse of the tunnel opening, i.e., the rigidity and state of the advance core played a determining role in the stability of the tunnel. These notions were also supported by the findings of Moritz et al. [11], who also concluded that the number and length of face bolts reduced surface settlements ahead of the tunnel face. In other words, the additional measures for face stabilization had a very positive impact on displacement behavior both in the tunnel and at ground surface. Hence from these results it appears that face extrusion, if measured, could be a good indicator for predicting the stability of deep tunnels and the potential loss of ground in the case of shallow tunnels.

2.2. Vector orientation

In tunnelling it is relatively easy to measure displacements of the tunnel crown. With the advent of precise geodetic measurements Schubert et al. [9] has suggested that these crown measurements when evaluated as a vector, provide valuable information on the the conditions ahead of the tunnel face,

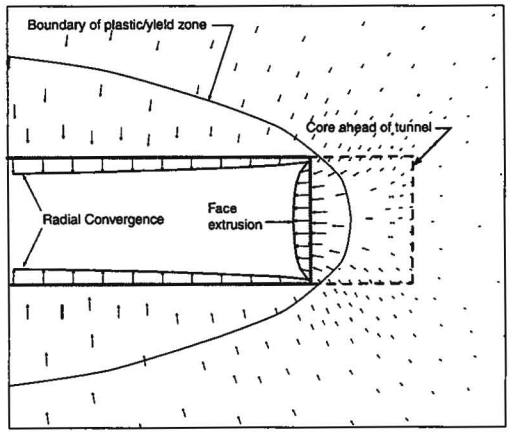

Fig. 2: Displacements near a tunnel face generated using an axis-symmetric model.

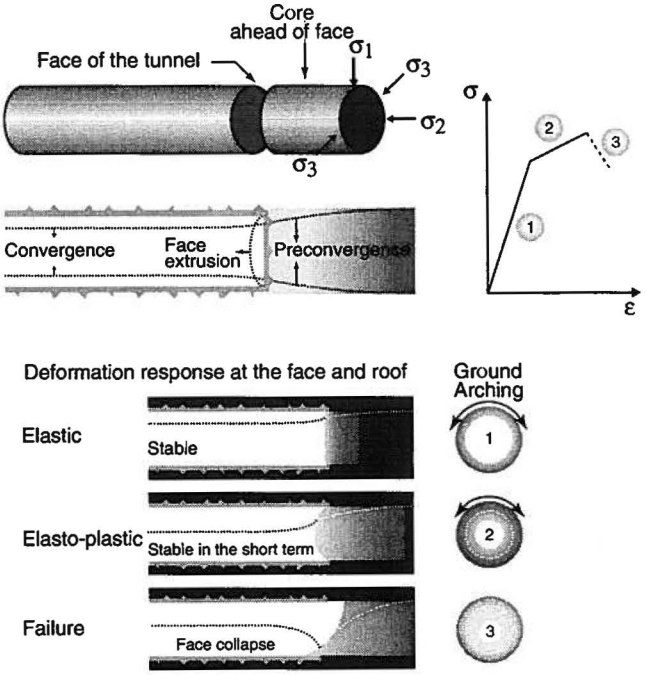

Fig. 3: Definitions of deformations and behavior of face advance core and tunnel roof (modified after Lunardi [8]).

as well as tunnel stability. The deformation vector evaluated by [9] is defined in Fig. 4. The vector orientation α is simply $\tan\alpha = \Delta L/\Delta S$. Schubert and Budil [1] noted that when a tunnel in relatively competent ground is approaching weak ground, stress concentrations develop in the stiffer ground. As a consequence Schubert and Budil [1] suggested that the longitudinal displacement (ΔL) would increase which leads to an increase of α. However, in case of a tunnel face approaching stiffer ground the opposite tendency occurs, i.e., the longitudinal displacement (ΔL) would decrease, with an accompanying decrease of α.

The early work to evaluate the changes in α to tunnel face conditions relied on the three-dimensional boundary element method assumming linear elastic material [1, 12, 13]. For many deep tunnelling projects this assumption may be valid. However, in weak rock the material response is often not elastic and an extensive plastic zone can develop around the tunnel. Particularly large tunnels such as those used for highway traffic. In the following sections the face extrusion concept proposed by [7] and the displacement vector concept proposed by [1] are evaluated using non-elastic numerical models.

3. *FLAC*3D model

To capture the effect of tunnel face extrusion and crown displacements a three-dimensional model is required. The three-dimensional finite difference software *FLAC3D*[1] was used for the analysis reported here.

A series of *FLAC3D* analysis were carried out to investigate changing ground conditions ahead of the tunnel face. Initial scoping calculations with different model geometries were carried out to ensure sufficiently accurate results [13]. The final model used was a 170-m-long tunnel consisting of 13,770 brick elements (Fig. 5). The circular tunnel has a diameter of 10 m with an outer boundary extending to a distance of 40 m perpendicular to the tunnel axis and 30 m to the vertical axis to minimize boundary effects. The models were divided into two regions (Region 1 and Region 2) with each region having different geotechnical properties. In the basic model (Fig. 5), Region 1 and Region 2 illustrate relatively stiff and weak ground, respectively. Tunnel excavation was carried out in a series of 2-m-long excavation steps.

The initial stress state was set to gravitational loading to simulate a shallow tunnel. For each step the excavation is advanced 2 m and support pressure is applied at specific distances from the tunnel face. The simulations were carried out to investigate the changes that occur to displacements (both in the vertical and longitudinal directions) and vector orientation at a monitoring point in the roof of a tunnel, and the displacements associated with face extrusion for various cases when the tunnel face is advancing towards weak ground. In this situation tunnelling is assumed to proceed horizontally from Region 1 to Region 2 (see Fig. 5). Several influences such as: ground material (linear elastic or elasto-plastic), the value of k_o, the stiffness ratio between the two regions, the length of the relatively weak ground, the orientation of the interface between the two regions, tunnel diameter, and non-homogeneity of geotechnical properties were considered in the numerical simulations.

[1]available from Itasca Consulting Group, Inc., Minneapolis, Minnesota, USA

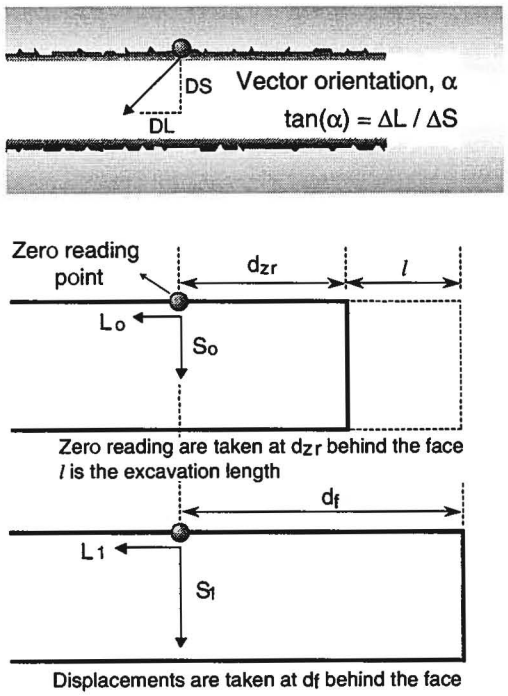

Fig. 4: Definition of the vector orientation (α) using an initial (zero) reading taken at some distance d_f from the tunnel face.

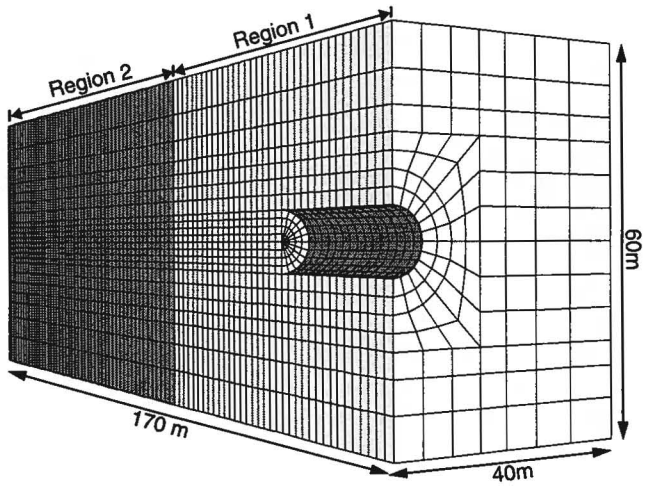

Fig. 5: The basic geometry included in the three-dimensional finite difference model *FLAC3D* .

Table 1 provides the geotechnical properties used in a *FLAC*3D models using both linear elastic and elasto-plastic constitutive models. The rock properties (A_1, A_2, P_1 and P_2) in Table 1 were developed using the Geological Strength Index (*GSI*) developed by [14]. The Mohr-Coulomb strength properties for each *GSI* class was developed using the procedure given in [15]. These properties are considered typical for a weathered rock mass and a weak rock mass in South Korea. The soil properties (P_3 and P_4) in Table 1 are also expressed in terms of the linear Mohr-Coulomb failure criterion. In all cases it was assumed that the weak rock and soil behaves as an elastic perfectly plastic medium.

4. Results from *FLAC3D* analyses

The deformations from numerical analyses include all the deformations associated with the application of the boundary conditions as well as the deformations due to the tunnel excavation. Monitoring displacements in the field, however, only shows a portion of the total displacement record because monitoring systems are usually installed inside the tunnels at a distance from the tunnel face. Hence, a portion of the total displacements caused by the tunnel excavation has already taken place prior to the beginning of monitoring. As a result, in the numerical models the zero reading is taken at a fixed distance from the tunnel face to simulate field monitoring conditions. Once the numerical monitoring begins the numerical results of vector orientations (α) with the tunnel face advance, ΔL and ΔS were calculated at each excavation step (Fig. 4).

4.1. Influence of weak ground ahead of tunnel face

The first series of simulations were carried out to investigate the influence of tunnelling from a competent rock mass (Region 1) toward a weak rock mass (Region 2). The geotechnical properties for Region 1 (A_2) and Region 2 (P_3) are given in Table 1. The ratio of horizontal stress to vertical stress, k_o value is 0.5 in both regions.

Table 1: Geotechnical properties used in three dimensional numerical simulations. The Geological Strength Index (*GSI*) was used to determine the cohesion and friction values. These properties reflect various ground classes encountered in South Korea.

	Weak/Weathered Rock Class				Soil Class	
	A_1	A_2	P_1	P_2	P_3	P_3
GSI	33	21	18	7		
σ_{ci} (MPa)	30	30	10	10		
σ_{cm} (MPa)	3.6	2.5	0.75	0.36		
E_m (MPa)	2000	1000	500	200	100	50
c (MPa)	0.40	0.30	0.15	0.09	0.05	0.005
$\phi(^\circ)$	38	33	27	22	20	30
ρ (kg/m^3)	2400	2400	2100	2100	2100	2100
ν	0.30	0.30	0.35	0.35	0.35	0.35

Fig. 6 shows the trend of the displacement at a point at the center of the tunnel crown located 2-m from the tunnel face. Fig. 6a gives the complete vertical settlements, i.e., includes the settlement that occurred ahead of the tunnel face. The results shown in Fig. 6a indicate that for this case where there is weak ground (Region 2) ahead of relatively stiff ground (Region 1), there is no significant increase in total vertical settlement until the tunnel reaches 0.4D from the beginning of the weak ground. This reflects the arching associated with the tunnel face.

Fig. 6b provides the displacement history familiar to most tunnelling engineers, i.e., the displacement history ahead of the tunnel face is not included. For this case fixed points

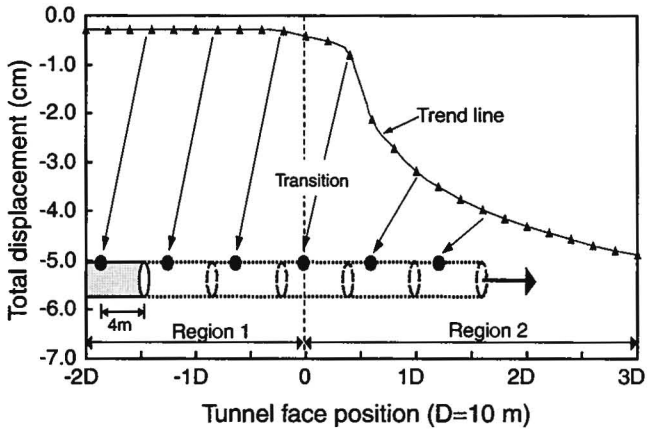

(a) Total vertical settlement plotted as a function of face position. The measurement point is located 2 m behind the tunnel face and for this case the displacement ahead of the tunnel face is included.

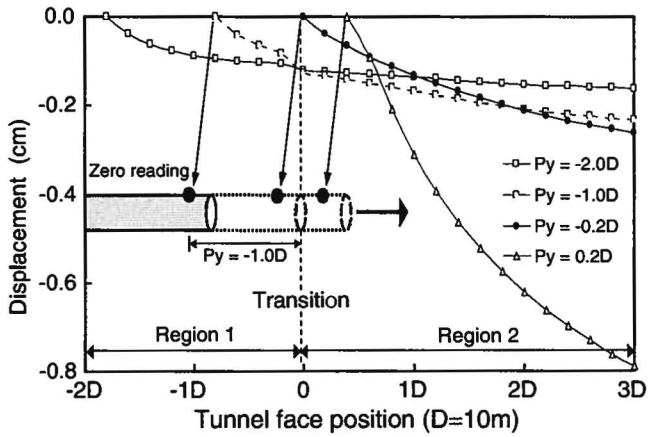

(b) Vertical settlement history for points installed 2 m from the tunnel face. For this case the displacement ahead of the tunnel face is not included.

Fig. 6: Displacements measured at 2 m increments from the tunnel face.

were chosen at Py=-2.0D, -1.0D, -0.2D and 0.2D, relative to the transition between Region 1 and Region 2 (Fig. 6b). The zero (initial) reading for each point was taken 2 m behind the tunnel face. For these situations there is no clear trend in the displacement patterns that would warn the tunnel engineer that the tunnel is approaching the weaker and softer ground. However, once the tunnel monitoring begins in the weaker ground, Py=0.2D, the displacements and the displacement rate are much larger. Thus the tunnel engineer should be alerted to changing ground conditions even if the tunnel face could not be observed. However, whether or not this additional convergence would lead to instability problems is a function of many additional parameters and hence evaluating this type of measurement data is often very difficult and requires considerable experience [16].

Fig. 7 shows a comparison between the trends observed for the vector orientation, $\Delta\alpha$, vertical settlement and extrusion with tunnel advance. Up to the station -2.0D (i.e. distance from the transition to tunnel face), no significant changes in vector orientations were observed and this value is considered the average vector orientation, $\Delta\alpha_{ave}$. Evaluation of data in Region 1 up to -2.0D shows that average

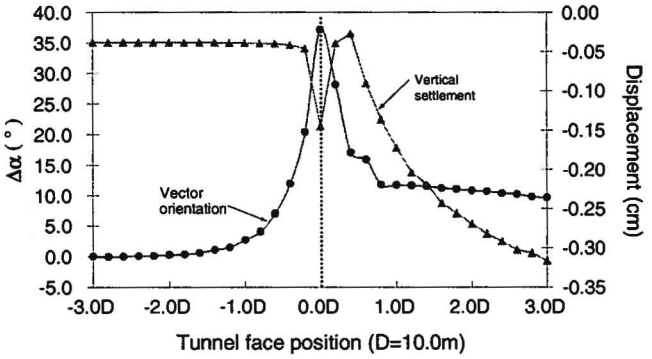

(a) Trend of vector orientation and increment of vertical settlement for points at the crown are 4.0 m behind the tunnel face (ko=0.5).

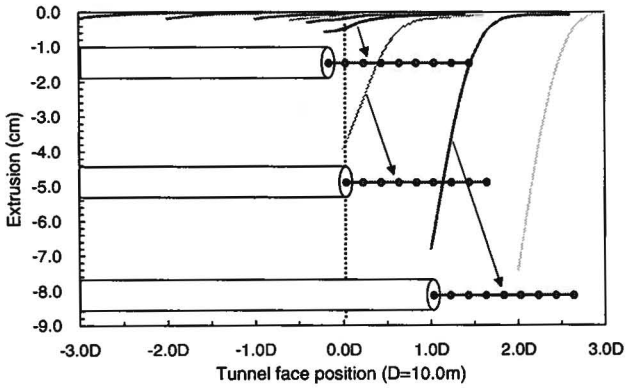

(b) Extrusions along horizontal distance from tunnel face

Fig. 7: Trend of displacement and vector orientation at crown, and face extrusion with tunnel advance.

vector orientation is approximately $-15°$. Schubert et al. [9] notes that average monitored angle between longitudinal displacement and crown settlement is between $-8°$ and $-12°$ from the evaluation of data taken from tunnels constructed in poor rock. In this paper, vector orientations, $\Delta\alpha$, are expressed relativel to the α_{ave}, i.e., $\Delta\alpha = \alpha - \alpha_{ave}$.

As the tunnel approaches the weak ground in Region 2, the relative increase in longitudinal displacements were considerably higher than the relative increase in radial displacements. As a result, with decreasing distance to the weak ground (Region 2), $\Delta\alpha$ increased significantly (Fig. 7a). Also shown in Fig. 7a is the vertical settlement caused by the tunnel. As shown in Fig. 7a the change in vertical settlement shows no significant change until the tunnel face has reached Region 2. Thus for this case, evaluating the vector orientation data would be provide advanced warning that changed ground conditions should be anticipated long before Region 2 was encountered by the tunnel face.

Fig. 7b shows the extrusion of the face as a function of face location. Face extrusion is not often measured because of the difficulty of having access to the tunnel face. In large tunnels a face-berm is often used to provide added support to the tunnel face rendering the tunnel face inaccessible. However, as shown in Fig. 7b if the face extrusion could be measured at regular intervals it would also provide advanced warning that the tunnel would intersect changing ground conditions.

As shown in Fig. 7, it is only the vector orientation that clearly changes well before the tunnel face intersects the weak ground. For these results the monitoring point was located 2 m from the tunnel face. Studies by Golser and Steindorfer [13] using elastic analysis, showed that the vector trend taken far from the tunnel face showed greater deviation than the trend taken near the tunnel face. Fig. 8 shows plots of vector orientation for crown monitoring points located at 2, 4, 6 and 8 m behind the tunnel face, i.e., d_f shown in Fig. 4. In these simulations, the results confirm

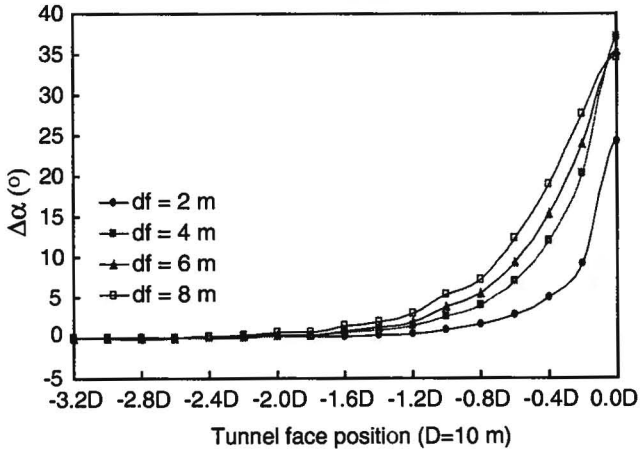

Fig. 8: Trends of $\Delta\alpha$ at the crown points 2, 4, 6 and 8 m behind the tunnel face.

the findings of Golser and Steindorfer [13]. However, while numerically such trends are observed, in the field it may not be practical to provide the accuracy required to measure the small displacements measured at large distances from the tunnel face.

4.2. Linear elastic and elasto-plastic behavior

A significant advantage of the Flac3D analysis compared to that of three dimensional boundary element solutions is the ability to model elasto-plastic material behavior. With the elastic solution, whether ground is weak or stiff, the displacements magnitudes are limited and the influence of yielding weak ground ahead of the tunnel face cannot be evaluated. Panet [4] notes that it is important to distinguish whether the plastic zone develops along the tunnel periphery behind the excavation face, or whether it encircles the excavation face thus endangering the stability of the face. In the following analyses the tunnel in Region 1 remains elastic, regardless of the constitutive model and hence the effect of the yield zone on vertical settlement, vector orientation and face extrusion can be observed in Region 2 where both the elastic and elasto-plastic behaviour is observed.

A comparison between the vertical settlement and vector orientation at the tunnel crown 4 m behind the tunnel face, and extrusion of the tunnel face were determined assuming linear elasticity and elasto-plastic yielding with the same geotechnical properties used previously above (Fig. 9). In all cases the displacements increase significantly as the tunnel approaches the weak ground when the elasto-plastic constitutive model is used.

Fig. 9a compares the results for vertical settlement using elasto-plastic and linear elastic material models. There is no significant difference in vertical settlement until the tunnel face is located approximately 0.6D, i.e. 6 m, in weak ground. For the elasto-plastic model, when the tunnel face is at 0.6D, the plastic zone extends approximately 5 m in the direction of radial and approximately and 8 m ahead of the tunnel face(Fig. 10).

Lunardi [7] notes that the stability of the tunnel can be evaluated by monitoring the deformation response ahead of the tunnel face (Fig. 3). Using both field experiments and laboratory tests, Lunardi [7] showed that there was a close correlation between the face deformations (extrusion) and the convergence behind the tunnel face. Figs. 9a and 9b supports the notion proposed by [7]. Thus, if the yielding in the weak ground is not detected early during the tunneling operations, a large plastic zone will develop ahead of the tunnel face (see Fig. 10). Controlling the deformations associated with this large yield zone may be very difficult.

Examination of the vector orientations in Fig. 9c show that plastic behavior starts to have a significant effect on the vector orientation when the tunnel face was approximately 4 m from the weak material. It is clear from Fig. 9 that the magnitude of the vertical settlement, vector orientation and face extrusion is significantly greater if yielding around the tunnel is included in the analyses. In the following sections other factors that may affect vector orientation are examined.

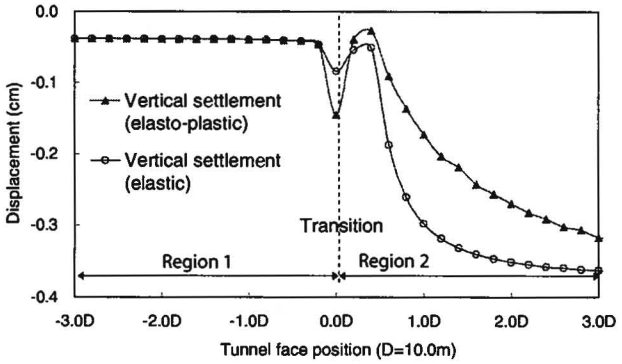

(a) Comparison of vertical settlement for an elastic and elasto-plastic model. The monitoring points at the crown are 4.0m behind the tunnel face (ko=0.5).

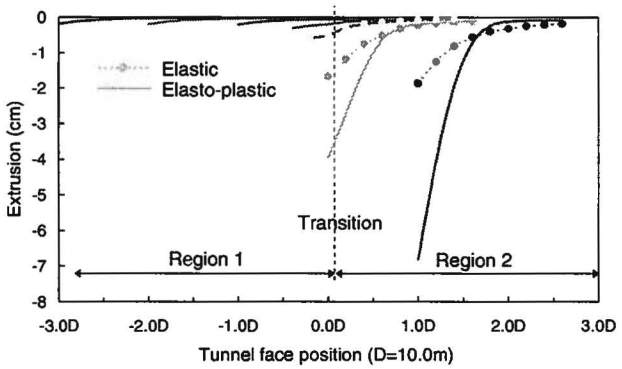

(b) Comparison of face extrusion for an elastic and elasto-plastic model.

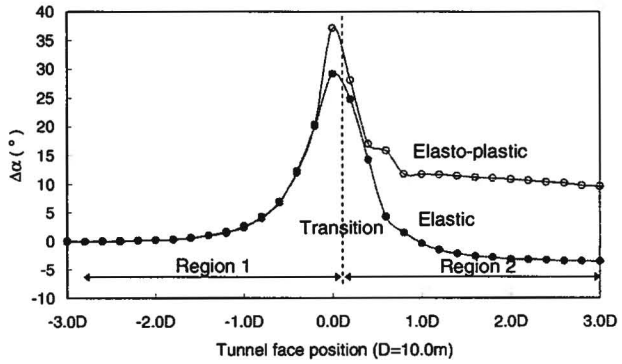

(c) Trends of $\Delta\alpha$ having different model at the crown points 4 m behind the tunnel face

Fig. 9: Displacement and vector orientation for elastic and elasto-plasto models.

4.3. In-situ stress state

A series of simulations were carried out to investigate the influence of initial in-situ stress state using geotechnical properties A_2 and P_3 shown in Table 1 for Region 1 and Region 2, respectively. In each case, the initial vertical stress was assumed to be equal to the weight of the overburden while the k_o values, i.e. horizontal/vertical stress ratio, were varied from k_o = 0.5, 0.75 and 1.0. In these analyses an elasto-plastic material model was used.

Fig. 11 provides plots of the vertical settlement, face extrusion and vector orientation for each of k_o values. Fig. 11a shows the results for the vertical settlement. For k_o = 0.5 and 0.75, there is essentially no difference in the amount of vertical settlement. The increase in vertical settlement for k_o = 1 is related to the development of a yield zone in the roof. When k_o = 0.5 and 0.75 the yield zone if it developed would occur locally on the sidewall of the tunnel and hence would not significantly affect the roof settlement. However, with k_o = 1 the yield zone extends around the entire tunnel, significantly increasing the roof settlement.

Fig. 11b shows the effect of the in-situ stress state on face extrusion. In all cases as the in-situ stress state increases from k_o = 0.5 to 1.0, the amount of face extrusion also increased. In Fig. 11c the vector orientation shows that as k_o increases the change in vector orientation occurs further from the beginning of Region 2. For example with k_o = 1, the change in vector orientation begins at about -1.8D while with k_o = 0.5 the change in vector orientation begins at about -1.2D. If the vector orientations are zeroed for each in-situ stress state, an increasing k_o tends to increase the maximum vector orientation value. Again, it is the influence of the k_o on the amount of yielding around the tunnel that determines its impact on vertical settlement, vector orientation and face extrusion.

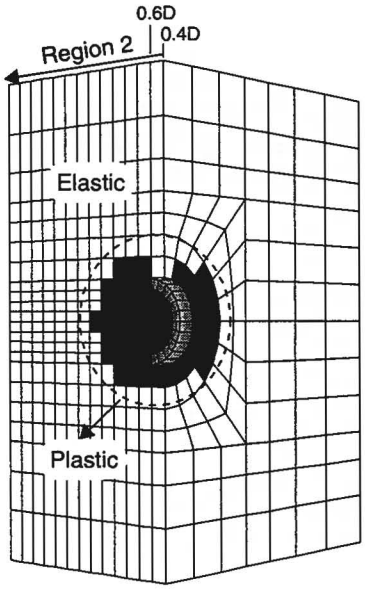

Fig. 10: Plots of the plastic zone around the tunnel face at 0.6D from the transition.

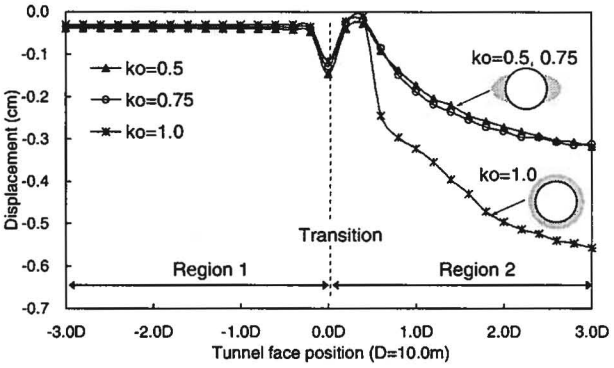

(a) Vertical settlement at the crown, 4.0m behind the tunnel face.

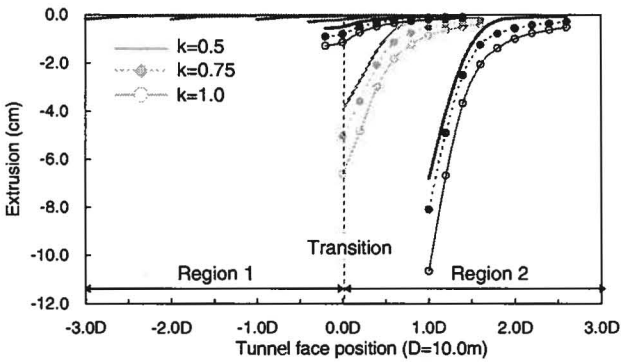

(b) Face extrusion

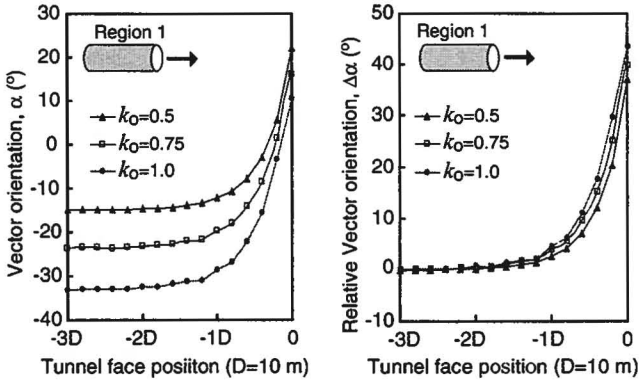

(c) Plots of vector orientation, α (left figure) and relative vector orientation, $\Delta\alpha$ (right figure).

Fig. 11: Plots of total vertical settlement, face extrusion and vector orientation having for in-situ stress state ranging from k_o = 0.5, 0.75 and 1.0.

Table 2: Geotechnical properties used in simulations, and computed vector orientation and extrusion.

Case	Property Classified in Table 1		SR	Vector orientation $\Delta\alpha^\circ$ at each station of the face				Tunnel face extrusion (cm) at each station of the face			
	Region 1	Region 2	E_{m1}/E_{m2}	-1D	-0.6D	-0.2D	0	-0.2D	0	0.4D	0.8D
I	A_2	P_1	2	0.8	2.2	5.9	14.3	0.27	0.39	0.41	0.42
II	A_2	P_2	5	2	5.3	14.5	30.5	0.43	1.32	1.67	1.77
III	A_2	P_3	10	2.7	7	20.4	37.2	0.57	3.95	5.88	6.61
IV	A_1	P_2	10	2.7	7	20.2	34.4	0.28	1.23	1.61	1.74
V	A_1	P_4	20	2.9	7.8	25.3	Failure	0.68	Failure	-	-
VI	A_1	P_3	20	2.9	7.8	25.2	39.0	0.34	3.75	5.79	6.57

4.4. Stiffness ratio

To investigate the influence of the stiffness ratio (SR), i.e., ratio of elastic modulus of Region 1 to Region 2, different elastic modulus and strength parameters for each regions were assumed. Table 2 summaries the geotechnical properties used in the numerical simulations with respect to the stiffness ratio adjacent two grounds. In addition, computed vector orientation 4m behind the tunnel face and extrusion at the tunnel face were provided in Table 2. The displacement measurements are taken at a distance 4m (0.4D) behind the tunnel face and k_o used in all simulations is 0.5.

The results show that, with increasing ratio of stiffness between two regions, the maximum deviation of the vector orientation, max, increased a little. In the case of assuming elasto-plastic behavior, however, it is hard to predict stiffness ratio between two regions in terms of the analysis of vector orientation only. As shown on Table 2, in Case III, IV, V and VI, deviation of the vector orientation seems to be similar before the tunnel face reaches the weak ground (i.e. station 0.0D) in spite of its different geotechnical properties. Although, in Case V, the failure occurred along the tunnel boundary followed formation of large plastic zone as the tunnel face approaches the weak ground, results of the vector orientation show similar trend as other case. In other words, trend of the vector orientation and vertical settlement only can't reflect instability of the ground with respect to accumulation of the plastic deformations, which initiate ahead of the tunnel face

Results for the extrusion on the tunnel face are seen to vary as condition for simulation though it has same stiffness ratio because extrusion depends on the strength and deformation properties of the ground ahead of the face and on the original stress field to which it was subject.

4.5. Length of relatively weak ground

A series of numerical simulations have been conducted to investigate the influence of the weak ground having different extensions shown in Fig. 12a, i.e., Ls=10 (1.0D), 20 (2.0D), 30 (3.0D), 50 (5.0D) and 100m (10.0D).

The results of total vertical settlement shown in Fig. 12b shows that tunnelling behind weak ground does not produce an increase in the settlements regardless of the weak ground's extension. In addition, the amount of total vertical settlement became smaller as the extension of the weak ground decreased. As a result, the numerical simulations show that the evaluation of trends of vertical settlement only, do not provide clear indication of weak ground or fault zone ahead of the tunnel face, because the increase of the absolute displacements may also be caused by a continuous increasing deformability of the ground.

Fig. 12c shows the trend of vector orientation. When the tunnel approaches the weak ground, the vector orientation showed an increasing trend against the direction of excavation. After the tunnel face entered the weak ground and approached the relatively stiff ground again, the vector orientation dropped down and recovered gradually. It is interesting to note that, regardless of the extension of the weak ground, the deviation of starts at a similar distance behind the weak ground and the maximum deviations of $\Delta\alpha$ almost appears to be similar. In more quantitative terms, the difference of max in cases of Ls=10 and 100m is less than 6°. Steindorfer [12] notes that a certain prediction of the extension of a fault zone as well as zones consisting of relatively weak ground ahead of the tunnel face is possible with the analysis of the vector orientation trends, as shown in Fig. 12c.

As described above, however, it depends on the amount of displacement in vertical and longitudinal direction as well as the initial stress state, Poisson's ratio, rock mass structure and such like. Therefore, it is not easy to predict the extension of the weak ground by $\Delta\alpha$ only in practice.

4.6. Tunnel diameter

It is known from the Kirsch equations that the amount of radial displacements around a circular opening is a function of the tunnel diameter, i.e., the large the diameter the greater the radial displacements. Tunnel diameters ranging from 5.0, 7.5 and 10.0 m, were used to investigate the influence of diameter on face extrusion and vector orientation. The tunnels were modelled with the in-situ vertical stress equal to the overburden stress and with $k_o = 0.5$. An elasto-plastic

material model was also used and each model had the same tunnel centerline coordinates. Accordingly, in each case, the in situ stress conditions were not identical as the distance from the roof of the tunnel to the ground surface varied.

The results for the relative vector orientation show that, with decreasing tunnel diameter, the maximum deviation of the vector orientation becomes larger and variation of the vector orientation starts a little earlier (Fig. 13a). This not so intuitive result occurs because for the longitudinal displacements remain relatively constant while the the radial displacements decrease as the tunnel diameter decreases. Because the monitoring point is 4 m from the tunnel face the tunnel convergence has not reached a maximum (see Fig. 2). Regardless of tunnel diameter the relative vector orientation shows the approaching weak ground in Region 2, before the tunnel face encounters it.

As expected the face extrusion increases as the tunnel diameter increases (Fig. 13b). These findings are similar to those of Hoek [8] who also showed using an axi-symmetric numerical model that face deformations tend to follow the trend of the radial displacements, which increase as the tunnel diameter increases.

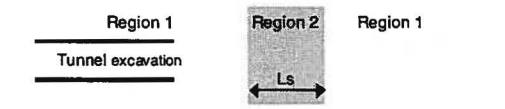

(a) Location of weak ground

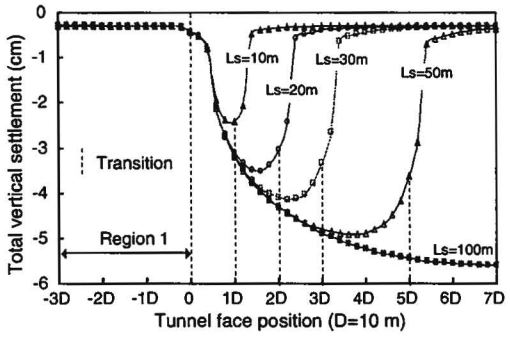

(b) Vertical settlement

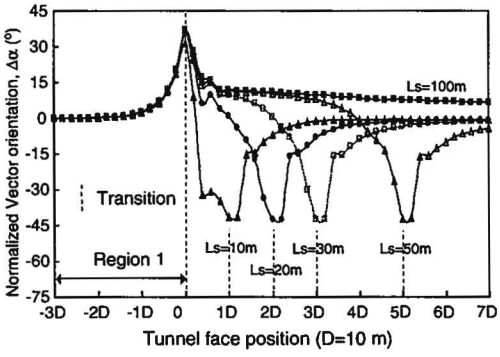

(c) Vector orientation

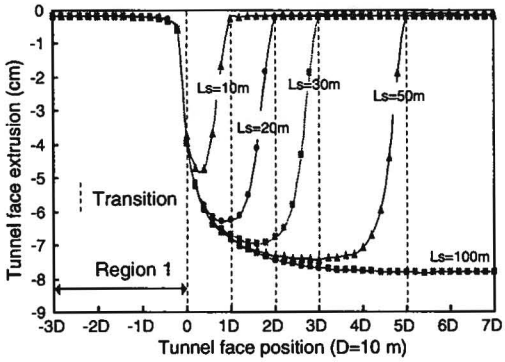

(d) Face extrusion

Fig. 12: Plots of displacements and vector orientation having different extensions of the weak ground (i.e. Region 2), L_s, for trends taken at 4 m behind the tunnel face and $k_o = 0.5$.

4.7. *Inclined interface*

In all the previous examples the transition interface between regions 1 and 2 was aligned perpendicular to the tunnel axis.

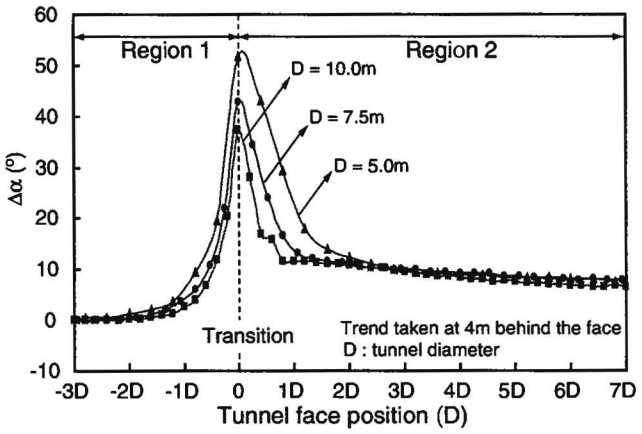

(a) Trends of $\Delta\alpha$ with different tunnel diameter (TD)

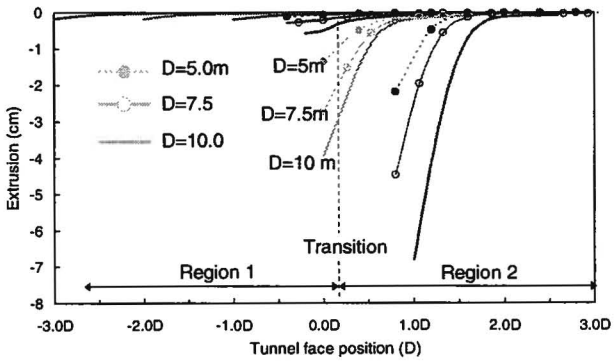

(b) Extrusion versus tunnel diameter (TD)

Fig. 13: Plots of vector orientation and extrusion having different tunnel diameter (D=5, 7.5 and 10 m).

In tunnelling this interface may be at any angle, depending on geological conditions. Numerical simulations were carried out with the inclination of the transition interface θ inclined at 90° and 45° with respect to tunnel axis. Geotechnical properties used in the simulations were A2 and P3 for Region 1 and Region 2, respectively. The properties for A2 and P3 are shown in Table 1. An elasto-plastic and elastic material model were used with $k_o = 0.5$. The elastic model was only used for teh 45° case as the results foo the 90° case were presented in Fig 9a

Comparisons of the vertical settlement, relative vector orientation and face extrusion for the various transition interfaces assuming linear elastic and elasto-plastic behaviour are shown in Fig. 14. Tunnel face position on the the x-axis in Fig. 14 represents a distance from centre of the transition interface to centre of the tunnel face.

Results for the vertical settlement show that when, when the transition interface is at an angle, vertical settlements become less reliable in predicting the presence of weak ground ahead of the tunnel face (Fig. 14a). However, the changes in the vector orientation become much more abrupt and clearly indicate changing ground conditions (see Fig. 14b). It is interesting to note that for an interface inclined at 45° the relative vector orientation is much more erratic compared to the vector orientation for $\theta = 90°$.

Fig. 14c shows the trend of face extrusion for the cases of $\theta = 45°$ in elastic material, and $\theta = 45°$ and $\theta = 90°$ in elasto-plastic material. The face extrusion results for the elasto-plastic model show similar trends regardless of inclination of the transition interface. Hence it would appear that while face extrusion shows much larger displacements in the weak ground only the relative vector orientation would provide information that might indicate that the orientation of the transition interface is not vertical.

4.8. Non-homogeneity

Steindorfer and Schubert [17] showed that when tunnelling through the Hinterberg fault zone in southern Austria, frequent changes in type and quality of rock caused a number of tunneling difficulties. Steindorfer and Schubert showed that the non-homogeneity of the ground frequently led to stress concentration and yielding in localized areas. In one case, Steindorfer and Schubert suggested that this overstressing led to a collapse of the tunnel crown. Steindorfer and Schubert showed that while the conventional evaluation of radial displacement data did not show any significant indication of the failure, analysis of the vector orientation showed significant variability. Steindorfer and Schubert concluded that vector orientation might be a useful indicator for quantifying heterogeneous ground.

In South Korea shallow tunnels often encounter heterogenous geology related to the formation of residual soil. In such geological conditions, geotechnical properties such as deformation modulus, cohesion and friction angle may be described as random variables. A series of Flac3D simulations were carried out to study the influence of material non-homogeneity on relative vector orientation and face extrusion.

The properties in Region 1 and Region 2 were specified to vary as function of grid position using a normal Gaussian distribution with a mean value μ and a standard deviation, S. In case of the Gaussian distribution, about 68% of the test values will fall within an interval defined by μ and $\pm S$ while approximately 95% of all the test results will fall within the range defined by the μ and $\pm 2S$. The coefficicnt of variance, COV, defined as the ratio of the standard deviation to the mean, is often used to express uncertainty in soil properties. Harr [18] suggest that COV for soils could vary

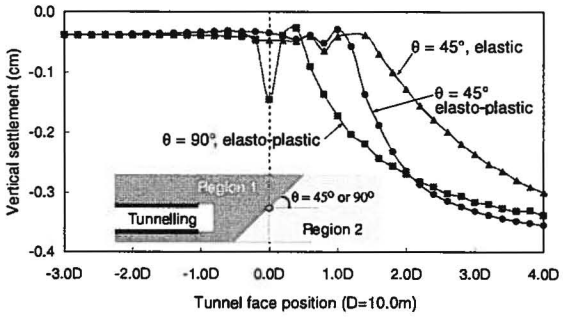

(a) Vertical settlement

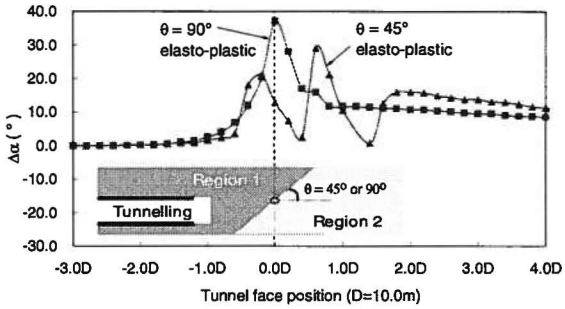

(b) Relative vector orientation

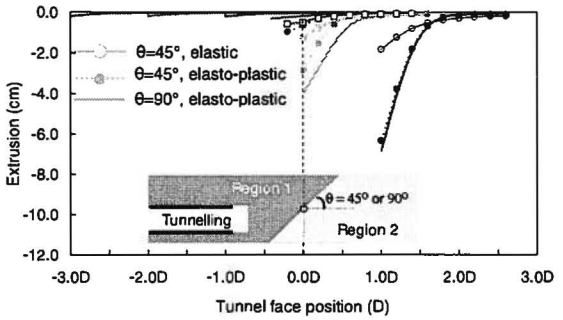

(c) Face extrusion

Fig. 14: Plots of displacements and vector orientation with the inclination of the transition interface sloped at $\theta = 45°$ and 90° with respected to the tunnel axis, assuming elasto-plastic and elastic material.

Table 3: Parameters for random input variables Random variables

Random variable	Region 1 Mean	Region 1 Std. Dev	Region 2 Mean	Region 2 Stdev
E_m (MPa)	1000	250	100	25
c (MPa)	0.3	0.045	0.05	0.0075
ϕ (°)	33	5	20	3

from 0.02 to 0.4. A small uncertainty would typically be represented by a COV=0.05 while considerable uncertainty would be indicated by a COV=0.25.

For the Flac3D simulations, the *COV* were assumed to be 0.25 for deformation modulus E_m and 0.15 for both cohesion (c) and friction angle (ϕ). Table 3 provides a summary of the mean and standard deviation used in the Flac3D simulations for each of these variables. The results from these analyses are summarized in Fig. 15

Fig. 15a compares the vector orientation for homogeneous geology with the transition inclined at $\theta = 45°$, to heterogeneous conditions with the same transition orientation. It

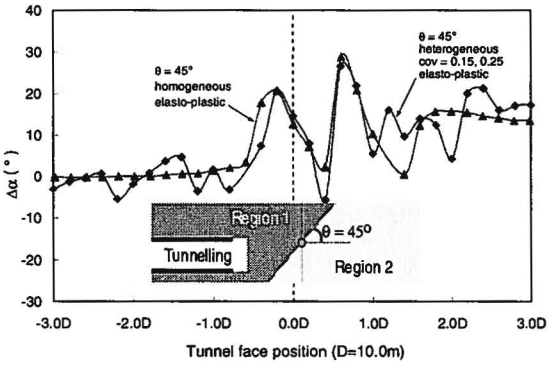

(a) Relative vector orientation

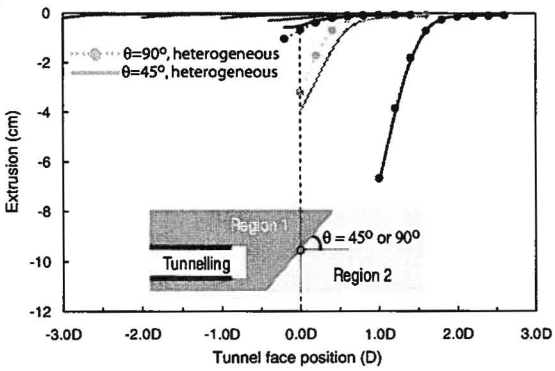

(b) Tunnel face extrusion

Fig. 15: Trends of vector orientation and extrusion with considering non-homogeneity of the ground in elasto-plastic material assuming that COV for elastic modulus in both Region 1 and Region 2 is 0.25, and for strength parameters is 0.15.

is clear from Fig. 15a that vector orientation varies significantly with heterogeneous soil conditions and that this variation increases as the weak ground condition in Region 2 is approached. Fig. 15b shows the face extrusion for heterogeneous soil conditions with a vertical and inclined transition zone. Comparing Fig. 15b with Fig. 14c shows that face extrusion is not sensitive to variability in the soil properties.

5. Discussion and Conclusions

Displacement monitoring plays a significant role in modern day tunnelling. With improvements in survey techniques displacements can now be routinely measured to ±0.1 mm in a typical tunnel construction environment. With this improvement in monitoring capability, there is an opportunity to advance our interpretation of these tunnel displacements beyond the traditional ground support interaction role. Schubert and Budil [1] showed that simple displacement monitoring of a point in the crown of a tunnel could provide information related to not only the ground support interaction but also changing ground conditions. This numerical study confirms Schubert and Budil [1] original hypothesis.

The *FLAC3D* analyses has shown that in all cases considered the vector orientation of a point in the crown of a tunnel provided information on the approaching ground conditions not readily observed in the traditional vertical/radial displacements or in face extrusion measurements. For simple geological conditions such as a tunneling towards an abrupt interface, the vector orientation gave ample warning of the approaching change in ground conditions. However, in more complex geological conditions such as frequently encountered in shallow tunnels interpretation of the vector orientation is more challenging. Nonetheless the rapid variation in the vector orientation in heterogeneous ground does point to changing ground conditions.

The results from these analyses suggests that vector orientation monitoring should be an essential tool for any tunnel monitoring program.

Acknowledgements

This work was conducted while the first author was visiting the Geotechnical Group at the University of Alberta. The support of the Hyundai Development Company during this visit is gratefully acknowledged.

References

1. Schubert W, Budil A, The importance of longitudinal deformation in tunnel excavation. In: Fujii T, editor, Proc. 8th, ISRM Congress on Rock Mechanics, Tokyo, vol. 3, Rotterdam: A.A. Balkema 1995 pp. 1411–1444.
2. Rabcewicz L, Stability of tunnels under rock load. Water Power 1969, 21(6):225–229.

3. Peck R B, Ninth Rankine Lecture: Advantages and limitations of the observational method in applied soil mechanics. Géotechnique 1969, 19(2):171–187.
4. Panet M, Understanding deformations in tunnels. In: Hudson J A, editor, Comprehensive Rock Engineering – Principles, Practice and Projects, vol. 1, Oxford: Pergamon Press 1993 pp. 663–690.
5. Fenner R, Undersuchungen zur erkenntnis des gebirgsdruckes. Gluckauf 1938, 74:681–695 and 705–715.
6. Lunardi P, Focaracci A, Giorgi P, Papacella A, Tunnel face reinforcement in soft ground: design and control during excavation. In: Proc. Towards New Worlds in Tunnelling, vol. 2, Rotterdam: A.A. Balkema 1992 pp. 897–908.
7. Lunardi P, Design and construction of tunnels using the approach based on the analysis of controlled deformation in rocks and soils. Tunnels and Tunnelling Int 2000, Special Supplement:3–30.
8. Hoek E, The Thirty Sixth Karl Terzaghi Lecture: Big tunnels in bad rock. J Geotech and Geoenviron Engin 2001, 127(9):726–740.
9. Schubert W, Steindorfer A, Button E A, Diplacement monitoing in tunnels - an overview. FELSBAU 2002, 20(2):7–15.
10. Schubert W, Steindorfer A, Advanced monitoring data evaluation and display for tunnels. In: Negro Jr A, Ferreira A A, editors, Proc. Int. Symp. Tunnels and Metropolises, Sao Paulo, vol. 2, Rotterdam: A.A. Balkema 1998 pp. 1205–1208.
11. Moritz B, Vergeiner R, Schubert P, Experience gained at monitoring of a shallow tunnel under a main railway line. FELSBAU 2002, 20(2):29–42.
12. Steindorfer A, Short term prediction of rock mass behaviour in tunnelling by advanced analysis of displacement monitoring data. Ph.D. thesis, Department of Civil Engineering, Graz University of Technology , Austria 1998.
13. Golser H, Steindorfer A, Displacement vector orientations in tunnelling - What do they tell? FELSBAU 2000, 18(2):16–21.
14. Marinos P, Hoek E, GSI: A geological friendly too for rock mass strength estimation. In: Proc. GeoEng2000, An International Conference on Geotechnical & Geological Engineering Melbourne, vol. 1: Invited Papers, Lancaster: Technomic Publishing Co., Inc 2000 pp. 1422–1440.
15. Hoek E, Carranza-Torres C, Corkum B, Hoek-Brown failure criterion - 2002 edition. In: Hammah R, Bawden W, Curran J, Telesnicki M, editors, Proc. 5th North American Rock Mechanics Symposium and 17th Tunnelling Association of Canada Conference: NARMS-TAC , Toronto, vol. 1, Toronto: University of Toronto Press 2002 pp. 267–273.
16. Rokahr R B, Stärk A, Zachow R, On the art of interpreting measurement results. FELSBAU 2002, 20(2):16–21.
17. Steindorfer A, Schubert W, Application of new methods of monitoring data analysis for short term prediction in tunnelling. In: Golser H, Hinkel W J, Schubert W, editors, Proc. Int. Symp. Tunnels for People, Vienna, Rotterdam: A.A. Balkema 1997 pp. 65–70.
18. Harr M E, Reliability-based Design in Civil Engineering. New York: McGraw Hill, Inc. 1987.